

Permeation in Gramicidin Ion Channels by Directly Estimating the Potential of Mean Force Using Brownian Dynamics Simulations

Vikram Krishnamurthy^{1,*}, Matthew Hoyles², Rayan Saab¹, and Shin-Ho Chung²

¹Department of Electrical and Computer Engineering, University of British Columbia, Vancouver, Canada

²Department of Theoretical Physics, Research School of Physical Sciences,
Australian National University, Canberra, Australia

We present a method for estimating the 'best-fit' potential of mean force encountered by an ion permeating across the gramicidin-A ion channel. The proposed method does not require explicit use of a dielectric constant and can be applied to other ion channels. The potential of mean force is parameterized and its parameters are estimated using a stochastic optimization algorithm that controls Brownian dynamics simulations. A loss function measuring the differences between currents simulated using Brownian dynamics and currents observed at various applied potentials and ionic concentrations is calculated to compare between possible candidate parameters of the potential of mean force. The results obtained indicate that several possible potentials of mean force with barrier-heights and well-depths in the vicinity of $6 kT$ and $4.5 kT$ provide optimal fits to the observed currents. Using both "brute-force" search and stochastic optimization, a sensitivity analysis is conducted to show the effect of potential of mean force (PMF) parameter variations on the simulated currents fit to the observables. We illustrate the methods using the gramicidin channel as a test case and show that the results closely match the profiles of potential of mean force reported in the literature.

Keywords: Adaptive Control, Brownian Dynamics, Stochastic Optimization, Stochastic Search Algorithms, Gramicidin Channels, Ion Permeation, Potential of Mean Force.

1. INTRODUCTION

One of the aims of constructing a theoretical model of an ion channel is to elucidate how individual ions propagate across the pore at a femtosecond time scale. The dimensions of certain constricted segments of typical ion channels are *mesoscopic*, in that the individual ions are comparable in radius to the ion channel. Inferences made from macroscopic electrostatics are valid only in the regions that are large compared to the diameters of ions and water molecules. In the narrow constricted region of the channel, whose radius may be nearly equal to or less than that of a monovalent ion with its first hydration shell, the representation of the dielectric as a continuous medium and an ion as a point charge may be a poor approximation.^{1,2}

Thus, there is a pressing question in applying electrostatics to a mesoscopic system that needs to be addressed. What is the value of the effective dielectric constant, ϵ_c , of the water-filled pore formed by a protein wall and does a

uniform value of ϵ_c exist at all? In the gramicidin channel, where the radius of the ion conducting path is only 2 \AA ,³⁻⁶ continuum electrostatics fails to describe ion permeation owing to the long single-file chain of water molecules in the pore.⁷ In the selectivity filter of the potassium channel, a potassium ion is solvated by carbonyl oxygen atoms and a water molecule at each end along the filter. Thus, Coulombic force experienced by the ion by other charged particles will be attenuated substantially. In other words, the effective dielectric constant ϵ_c , if one exists, is likely to be higher than that in the interior of the protein, but the precise value to be used for solving Poisson's equation is not yet determined.

Here we present a method of estimating the PMF for any arbitrary channel based on a stochastic optimization algorithm. Given a three-dimensional shape of the pore and experimentally-determined currents across the channel under various conditions, our scheme calculates the PMF encountered by permeating ions that minimizes the discrepancies between measured and simulated currents. We first make a guess of several feasible PMF's that are

*Author to whom correspondence should be addressed.

parameterized by mixtures of Gaussian basis functions. After randomly selecting one such PMF as our initial guess, the target currents at different applied potentials and different ionic concentrations are specified, and the results of the simulations obtained by using the initial, guessed PMF are compared with the target currents. The stochastic search algorithm then evaluates the loss function between the two sets of measurements and modifies the parameters of the Gaussian mixture to be used in the next iteration. This process is repeated many times until the updated PMF converges. We illustrate this method for deducing the profile of the PMF encountered by a sodium ion as it traverses across the gramicidin pore.

The equilibrium PMF calculated in this way, using the adaptive controlled Brownian dynamics, incorporates the atomic fluctuations, which are believed to be intrinsic features of any channel proteins. The profile also incorporates the effective dielectric constant of the pore. Because the profile is engineered to match all the macroscopic observables, it reflects the closest approximation within a class of functions to the true force encountered by a permeating ion at each discrete conduction step across the molecular pore.

The paper is organized as follows. We first give the formalism of the Brownian dynamics algorithm, which can be construed as a continuous-time stochastic dynamical system satisfying the Langevin equation. Then, we introduce a novel, learning-based dynamic algorithm for estimating the profile of PMF, which we call adaptive controlled Brownian dynamics. Adaptive controlled Brownian dynamics entails the use and evaluation of a loss function in which we incorporate some prior knowledge, namely the linearity of the current–voltage curve in gramicidin-A. We report our results on the optimal PMF as well as on the loss surface for all candidate PMF's obtained using the proposed algorithm. We compare these results to the analogous results obtained using a brute-force search approach conducted on a grid of parameters, and note that both approaches agree on the optimal PMF and on the loss surface. We also observe that there are several PMF's with low values of the loss function, indicating that possibly more than one set of parameters can produce conduction that fits the observables well.

2. OVERVIEW OF BROWNIAN DYNAMICS

We first outline the traditional Brownian dynamics method for estimating ionic currents across a model channel and compare it with the new method we introduce, which we call *adaptive controlled Brownian dynamics*.

The computational steps involved in the Brownian dynamics algorithm are as follows. First, initial estimates of the structural information of the channel, namely, the channel geometry and charges on the ionizable residues in the protein, are used to determine the parameters of Poisson's equation. Numerically solving Poisson's equation yields the energy profile or PMF an ion traveling through the ion channel will experience. This in turn feeds

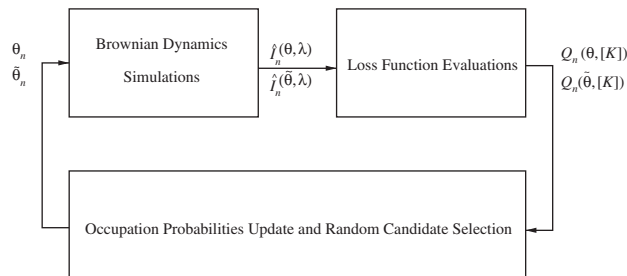


Fig. 1. Block diagram of the adaptive controlled Brownian dynamics algorithm.

into the Brownian dynamics simulation that governs the stochastic evolution of all the ions. As a result of ions modeled by Brownian dynamics permeating through the ion channel, a simulated ion channel current is obtained. This simulated ion channel current is compared with the experimentally observed ion channel current. The difference between the two currents is used to refine or modify the model of the channel geometry and charges and the process is repeated until the error between the simulated (predicted) ion channel current and experimentally determined ion channel current is minimized.

The method of adaptive, controlled Brownian dynamics we propose here is designed to circumvent the limitations posed by the traditional simulation approach outlined above. In this method, we solve the inverse problem. That is, given the 3-dimensional shape of a channel, we deduce the potential of mean force encountered by an ion traversing the channel that correctly replicates the experimental findings. To achieve this aim, we first make a guess of several feasible PMF's, representing each with a Gaussian basis function characterized by a multi-dimensional parameter vector. We then randomly select one of them as our initial guess and successively refine the initial guess using a stationary stochastic optimization algorithm. In this way, we derive the PMF that minimizes the mean square error between the simulated current and the actual observed experimental current. The steps involved in this algorithm are schematically shown in Figure 1.

2.1. The Brownian Dynamics Formalism

To make this paper self-contained, we briefly overview the notation and the setup of the simulation assembly. We also give a complete formulation of the permeation of ions across the membrane pore as a continuous-time stochastic dynamical system that satisfies the Langevin equations.

Two reservoirs \mathcal{R}_1 and \mathcal{R}_2 are connected to the ion channel \mathcal{C} . Each reservoir comprises of N K^+ ions (indexed by $i = 1, 2, \dots, N$) and N Cl^- ions (indexed by $i = N + 1, \dots, 2N$). Let $t \geq 0$ denote continuous time. With no loss of generality, throughout we illustrate our scheme using the gramicidin-A channel as an example. An external potential $\Phi_\lambda^{\text{ext}}(\mathbf{x})$ is applied along the z axis of the setup, i.e., with $\mathbf{x} = (x, y, z)$, $\Phi_\lambda^{\text{ext}}(\mathbf{x}) = \lambda z$, $\lambda \in \Lambda$. Due to

this applied potential, K^+ ions drift across the ion channel. Let $\mathbf{X}_t = (\mathbf{x}_t^{(1)'}, \mathbf{x}_t^{(2)'}, \mathbf{x}_t^{(3)'}, \dots, \mathbf{x}_t^{(2N)'})' \in \mathcal{R}^{2N}$ denote the positions and $\mathbf{V}_t = (\mathbf{v}_t^{(1)'}, \mathbf{v}_t^{(2)'}, \mathbf{v}_t^{(3)'}, \dots, \mathbf{v}_t^{(2N)'})' \in \mathbb{R}^{6N}$ denote the velocities of all the $2N$ ions. The position $\mathbf{x}_t^{(i)} = (x_t^{(i)}, y_t^{(i)}, z_t^{(i)})'$ and velocity $\mathbf{v}_t^{(i)}$ of each of $2N$ ions in the simulation assembly evolves as

$$\mathbf{x}_t^{(i)} = \mathbf{x}_0^{(i)} + \int_0^t \mathbf{v}_s^{(i)} ds \quad (1)$$

$$m^+ \mathbf{v}_t^{(i)} = m^+ \mathbf{v}_0^{(i)} - \int_0^t m^+ \gamma^+(\mathbf{x}_s^{(i)}) \mathbf{v}_s^{(i)} ds + \int_0^t F_{\theta, \lambda}^{(i)}(\mathbf{X}_s) ds + \int_0^t b^+(\mathbf{x}_s^{(i)}) d\mathbf{w}_s^{(i)}, \quad i \in \{1, 2, \dots, N\} \quad (2)$$

$$m^- \mathbf{v}_t^{(i)} = m^- \mathbf{v}_0^{(i)} - \int_0^t m^- \gamma^-(\mathbf{x}_s^{(i)}) \mathbf{v}_s^{(i)} ds + \int_0^t F_{\theta, \lambda}^{(i)}(\mathbf{X}_s) ds + \int_0^t b^-(\mathbf{x}_s^{(i)}) d\mathbf{w}_s^{(i)}, \quad i \in \{N+1, N+2, \dots, 2N\} \quad (3)$$

where the frictional coefficient $m^\pm \gamma^\pm(\mathbf{x}_s^{(i)}) = m^\pm \gamma^\pm = \frac{kT}{D^\pm}$, if $\mathbf{x}_s^{(i)} \in \mathcal{R}_1 \cup \mathcal{R}_2$. Here $D^+ = 1.96 \times 10^{-9}$ m²/s is the diffusion coefficient of K^+ ions within a bulk solution, and $D^- = 2.03 \times 10^{-9}$ m²/s is the diffusion coefficient for Cl^- ions.

Equations (2) and (3) are the *Langevin* equations. The process $\mathbf{w}_t^{(i)}$ denotes a 3-dimensional Brownian motion, which is component-wise independent. The terms $b^+(\mathbf{x}_s^{(i)})$ and $b^-(\mathbf{x}_s^{(i)})$ are, respectively,

$$b^+(\mathbf{x}_s^{(i)}) = 2m^+ \gamma^+(\mathbf{x}_s^{(i)}), \quad b^-(\mathbf{x}_s^{(i)}) = 2m^- \gamma^-(\mathbf{x}_s^{(i)}) \quad (4)$$

Finally, the noise processes $\mathbf{w}_t^{(i)}$ and $\mathbf{w}_t^{(j)}$, that drive any two different ions, $j \neq i$, are assumed to be statistically independent. Here, $F_{\theta, \lambda}^{(i)}(\mathbf{X}_t) = -q^{(i)} \nabla_{\mathbf{x}_t^{(i)}} \Phi_{\theta, \lambda}^{(i)}(\mathbf{X}_t)$ represents the systematic force acting on ion i , where the scalar valued process $\Phi_{\theta, \lambda}^{(i)}(\mathbf{X}_t)$ is the total electric potential experienced by ion i given the position \mathbf{X}_t of the $2N$ ions. The subscript λ is the applied external potential. The subscript θ is a parameter vector that characterizes the PMF defined below. To implement the above system on a digital computer we utilize a discretized version of the above equations.

The potential $\Phi_{\theta, \lambda}^{(i)}(\mathbf{X}_t)$ experienced by each ion i comprises of the following five components:

$$\Phi_{\theta, \lambda}^{(i)}(\mathbf{X}_t) = U_\theta(\mathbf{x}_t^{(i)}) + \Phi_\lambda^{\text{ext}}(\mathbf{x}_t^{(i)}) + \Phi^{\text{IW}}(\mathbf{x}_t^{(i)}) + \Phi^{C, i}(\mathbf{X}_t) + \Phi^{\text{SR}, i}(\mathbf{X}_t) \quad (5)$$

Here $U_\theta(\mathbf{x}_t^{(i)})$ denotes the PMF, $\Phi_\lambda^{\text{ext}}(\mathbf{x}_t^{(i)})$ denotes the external potential applied along the z axis of the gramicidin-A channel, $\Phi^{\text{IW}}(\mathbf{x}_t^{(i)})$ denotes the ion-wall interaction potential, also called the σ/r^9 potential, $\Phi^{C, i}(\mathbf{X}_t)$ denotes the inter-ion Coulomb potential and $\Phi^{\text{SR}, i}(\mathbf{X}_t)$ denotes the short range ion-ion potential. The PMF U_θ

is a smooth function of the ion position $\mathbf{x}_t^{(i)}$ and depends on the structure of the ion channel. Therefore, estimating $U_\theta(\cdot)$ yields structural information about the ion channel. For the gramicidin-A channel, we will represent $U_\theta(\cdot)$ by a Gaussian mixture with parameter vector θ and then present a stochastic algorithm to estimate θ .

2.2. Systematic Force Acting on Ions

As mentioned after Eq. (4), the systematic force experienced by each ion i is

$$F_{\theta, \lambda}^{(i)}(\mathbf{X}_t) = -q^{(i)} \nabla_{\mathbf{x}_t^{(i)}} \Phi_{\theta, \lambda}^{(i)}(\mathbf{X}_t)$$

where the scalar valued process $\Phi_{\theta, \lambda}^{(i)}(\mathbf{X}_t)$ denotes the total electric potential experienced by ion i given the position \mathbf{X}_t of all the $2N$ ions.

Just as $\Phi_{\theta, \lambda}^{(i)}(\mathbf{X}_t)$ is decomposed into 5 terms, we can similarly decompose the force $F_{\theta, \lambda}^{(i)}(\mathbf{X}_t) = -q \nabla_{\mathbf{x}_t^{(i)}} \Phi_{\theta, \lambda}^{(i)}(\mathbf{X}_t)$ experienced by ion i as the superposition (vector sum) of 5 force terms, where each force term is due to the corresponding potential in Eq. (5)—however, for notational simplicity we describe the scalar valued potentials rather than the vector valued forces.

Note that the first three terms in Eq. (5), namely $U_\theta(\mathbf{x}_t^{(i)})$, $\Phi_\lambda^{\text{ext}}(\mathbf{x}_t^{(i)})$, $\Phi^{\text{IW}}(\mathbf{x}_t^{(i)})$ depend only on the position $\mathbf{x}_t^{(i)}$ of ion i , whereas the last two terms in Eq. (5) $\Phi^{C, i}(\mathbf{X}_t)$, $\Phi^{\text{SR}, i}(\mathbf{X}_t)$ depend on the distance of ion i to all the other ions, i.e., the position \mathbf{X}_t of all the ions. We will now define the potential of mean force in Eq. (5).

Potential of mean force (PMF), denoted $U_\theta(\mathbf{x}_t^{(i)})$ in Eq. (5), comprises of electric forces acting on ion i when it is in or near the ion channel. The PMF U_θ is a smooth function of the ion position $\mathbf{x}_t^{(i)}$ and depends on the structure of the ion channel. Therefore, estimating $U_\theta(\cdot)$ yields structural information about the ion channel. The main aim of paper is to estimate the PMF $U_\theta(\cdot)$. Indeed, we will represent $U_\theta(\cdot)$ by a Gaussian mixture with parameter vector θ and then present a provably convergent stochastic algorithm to estimate θ .

The PMF U_θ originates from two different sources. First, there are fixed charges in the channel protein and the electric field emanating from them renders the pore attractive to one ionic species and repulsive to another. Some of the amino acids forming the ion channels carry the unit or partial electronic charges. Secondly, when any of the ions in the assembly comes near the protein wall, it induces surface charges of the same polarity at the water-protein interface. This is known as the induced surface charges.

2.3. Brownian Dynamics Algorithm

We run the BD simulation algorithm for L iterations. Each iteration proceeds until an ion crosses the channel. We denote these random times as $\hat{\tau}_{\mathcal{R}_1, \mathcal{R}_2}^{(l)}$ if the ion has crossed from \mathcal{R}_1 to \mathcal{R}_2 and $\hat{\tau}_{\mathcal{R}_2, \mathcal{R}_1}^{(l)}$ if the ion has crossed from \mathcal{R}_2

to \mathcal{R}_1 . We also count the number of times $L_{\mathcal{R}_1, \mathcal{R}_2}$ that K^+ ions have crossed from \mathcal{R}_1 to \mathcal{R}_2 , and the number of times $L_{\mathcal{R}_2, \mathcal{R}_1}$ that K^+ ions have crossed from \mathcal{R}_2 to \mathcal{R}_1 . Note that $L_{\mathcal{R}_1, \mathcal{R}_2} + L_{\mathcal{R}_2, \mathcal{R}_1} = L$. We only consider passage of positive K^+ ions $i = 1, \dots, N$ across the ion channel since in a cationic channel the ion channel current is caused only by positive ions. Finally, we compute the mean first passage time and mean current estimate after L iterations as

$$\hat{\tau}_{\mathcal{R}_1, \mathcal{R}_2}^{(\theta, \lambda)}(L) = \frac{1}{L_{\mathcal{R}_1, \mathcal{R}_2}} \sum_{l=1}^{L_{\mathcal{R}_1, \mathcal{R}_2}} \hat{\tau}_{\mathcal{R}_1, \mathcal{R}_2}^{(l)} \quad (6)$$

$$\hat{\tau}_{\mathcal{R}_2, \mathcal{R}_1}^{(\theta, \lambda)}(L) = \frac{1}{L_{\mathcal{R}_2, \mathcal{R}_1}} \sum_{l=1}^{L_{\mathcal{R}_2, \mathcal{R}_1}} \hat{\tau}_{\mathcal{R}_2, \mathcal{R}_1}^{(l)}$$

$$\hat{I}^{(\theta, \lambda)}(L) = q^+ \left(\frac{1}{\hat{\tau}_{\mathcal{R}_1, \mathcal{R}_2}^{(\theta, \lambda)}(L)} - \frac{1}{\hat{\tau}_{\mathcal{R}_2, \mathcal{R}_1}^{(\theta, \lambda)}(L)} \right) \quad (7)$$

In terms of the mean first passage times $\tau_{\mathcal{R}_1, \mathcal{R}_2}^{(\theta, \lambda)}$, $\tau_{\mathcal{R}_2, \mathcal{R}_1}^{(\theta, \lambda)}$, the mean current flowing from \mathcal{R}_1 via the gramicidin-A channel \mathcal{C} into \mathcal{R}_2 is defined as

$$I^{(\theta, \lambda)} = q^+ \left(\frac{1}{\tau_{\mathcal{R}_1, \mathcal{R}_2}^{(\theta, \lambda)}} - \frac{1}{\tau_{\mathcal{R}_2, \mathcal{R}_1}^{(\theta, \lambda)}} \right) \quad (8)$$

However, it is not possible to obtain explicit closed form expressions for $I(\theta)$ in Eq. (8). The aim of Brownian dynamics simulation is to obtain estimates of these quantities by directly simulating the stochastic dynamical system of Eqs. (1), (2), and (3). In particular, the following result, the proof of which is given by Krishnamurthy and Chung,⁸ shows that the estimated current $\hat{I}^{(\theta, \lambda)}(L)$ obtained from the above Brownian dynamics simulation algorithm is strongly consistent.

Theorem 1. For fixed PMF $\theta \in \Theta$ and applied external potential $\lambda \in \Lambda$, the ion channel current estimate $\hat{I}^{(\theta, \lambda)}(L)$ obtained from the Brownian dynamics simulation algorithm over L iterations is strongly consistent, i.e.,

$$\lim_{L \rightarrow \infty} \hat{I}^{(\theta, \lambda)}(L) = I^{(\theta, \lambda)} \quad \text{w.p.1} \quad (9)$$

where $I^{(\theta, \lambda)}$ is the mean current defined in Eq. (8).

3. ADAPTIVE CONTROLLED BROWNIAN DYNAMICS

3.1. Formulation of PMF Estimation Problem

With the above setup summarized briefly in the previous section, we are now ready to tackle our main goal of estimating the PMF U_θ of a gramicidin-A channel. We first approximate the PMF U_θ with a finite basis function approximation. Here we chose the basis functions to be a mixture of Gaussian functions that is characterized by a 5-dimensional parameter vector θ . Then we formulate the

PMF estimation problem as a stationary stochastic optimization problem. We also give an explicit construction of how the simulated current through the ion channel can be computed via Brownian dynamics simulation. The main contribution below is to formulate the problem of estimating the PMF U_θ as a discrete stochastic optimization problem involving minimizing the mean square error between the Brownian dynamics simulated current ($\hat{I}_T(\theta, \lambda)$) and the actual observed experimental current I .

3.2. Parameterization of Gramicidin-A Channel PMF with Gaussian Mixture

The PMF $U_\theta(\mathbf{x})$ of the gramicidin-A channel can be approximated with a Gaussian basis function. The PMF structure of the gramicidin-A channel is well known.⁹⁻¹³ Hence a basis function approximation of the gramicidin-A PMF $U_\theta(\mathbf{x})$ needs to capture the following important properties of the gramicidin-A channel:

(1) The K^+ ion moves along the center of the ion channel, i.e., its coordinates $\mathbf{x} = (x, y, z) = (0, 0, z)$. The PMF $U_\theta(\mathbf{x})$ (where $\mathbf{x} = (0, 0, z)$) experienced by the ion within the gramicidin-A channel is symmetric with respect to z , i.e.,

$$U_\theta(\mathbf{x}) = U_\theta(0, 0, z) = U_\theta(0, 0, -z) \quad \text{for all } \mathbf{x} \in \mathcal{C}$$

(2) For $z < -20 \text{ \AA}$ or $z > 20 \text{ \AA}$, $U_\theta(0, 0, z)$ should be close to 0—since the PMF only acts on ions in or near the ion channel.

Since the PMF $U_\theta(\mathbf{x})$ is a continuously differentiable function of \mathbf{x} , it can be uniformly approximated arbitrarily closely by a set of Gaussian basis functions or some other radial basis function. By using physiological data of the gramicidin-A channel, we find that the following scaled Gaussian mixture comprising of a linear combination of 3 Gaussian density functions gives an excellent fit:

$$U_\theta([0, 0, z]) = m \exp\left(-\frac{1}{2} \frac{(z-W)^2}{\sigma^2}\right) + m \exp\left(-\frac{1}{2} \frac{(z+W)^2}{\sigma^2}\right) + m_0 \exp\left(-\frac{1}{2} \frac{z^2}{\sigma_0^2}\right) \quad (10)$$

where

$$\theta = (W, \sigma^2, m, \sigma_0^2, m_0)' \quad (11)$$

The above Gaussian mixture comprises of two Gaussian functions with identical weighting factors m and identical variance σ^2 , centered about $z = W$ and $z = -W$, respectively—and a third zero mean Gaussian centered about $z = 0$ with variance σ_0^2 and weighting factor m_0 . It is obvious that the above parameterization satisfies the symmetry property 1 above. Also for suitable choice of the parameter vector θ in Eq. (11), property 2 holds.

It is worth noting that by using a linear combination of more than 3 Gaussian basis functions parameterized appropriately, one could approximate the PMF arbitrarily

closely. However, using 3 Gaussian basis functions seems to provide a good compromise between quality of fit and the complexity of the optimization problem to be solved.

The structure of the gramicidin-A channel, implies that the parameters θ defined in Eq. (11) need to be constrained to the set Θ defined as follows:

$$\Theta = \{\theta: W \in [0, 30 \text{ \AA}], \quad \sigma^2 \in [0, \sigma_{\max}^2], \quad m \in [0, M], \\ \sigma_0^2 \in [0, \sigma_{\max}^2], \quad m_0 \in [0, M]\} \quad (12)$$

where M and σ_{\max} are positive bounded constants.

Edwards et al.⁷ deduce the PMF for the gramicidin-A channel, which when incorporated into a non-equilibrium permeation model, best fits the observed physiological data. Their best-fit PMF U_θ , fitted with the Fermi function, has two potential wells of 7 kT along the z -axis, one at $z = -9 \text{ \AA}$, the other at $z = 9 \text{ \AA}$. Also at $z = 0$, the potential barrier is 5 kT (with respect to the potential wells). For mathematical convenience, we fit U_θ with a mixture of Gaussian basis functions (Eq. (10)). Using the Nelder-Mead simplex (direct search) optimization algorithm in Matlab, we obtained the best least squares fit over the interval $z \in [-20 \text{ \AA}, 20 \text{ \AA}]$ as

$$\theta^* = (9.00, 16.00, -7.11, 12.25, -1.41)' \quad (13)$$

Figure 2 shows the PMF generated by the Gaussian mixture approximation Eq. (10) with parameter θ^* .

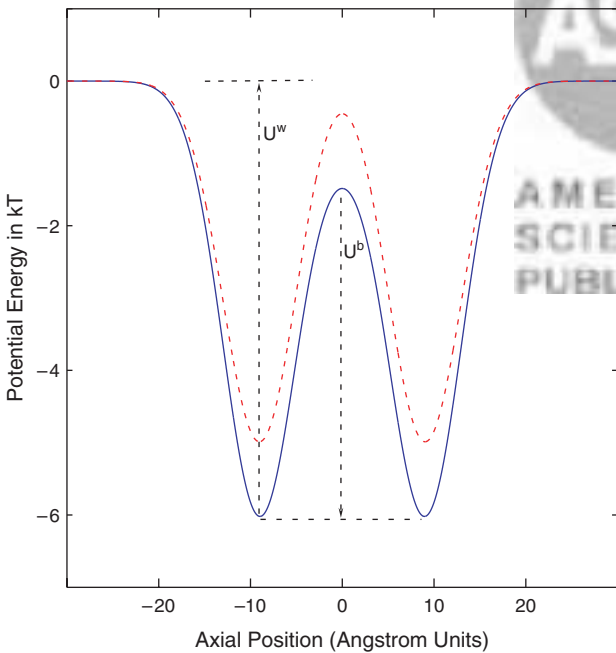


Fig. 2. PMF U_θ of gramicidin-A ion channel obtained by a 3 component Gaussian mixture. The two basic parameters characterizing $U_\theta([0; 0; z])$ are the depths of the two wells U^w and the height of the barrier U^b . The width of the barrier is approximately 10 \AA . The PMF shown (solid curve) with $U^w = 6 \text{ kT}$ and $U^b = 4.5 \text{ kT}$ gives the best description of the physiological data on gramicidin-A ion channels, while the PMF (dashed curve) with $U^w = 5 \text{ kT}$ and $U^b = 4.5 \text{ kT}$ is the state of the algorithm after 3 iterations.

3.3. Parameterization of Multi-Ion Channel PMF with Gaussian Mixture

So far we have assumed a single ion channel, i.e., that only one ion travels through the ion channel at any given time instant. However, in more complicated ion channels typically two, three, or more ions can be present in the ion channel simultaneously. The purpose of this subsection is to show that subject to some minor modifications, the single ion PMF can still be used to characterize the PMF of multi-ion channels.

Assume that the shape and structure of the channel are not altered by the presence of a second ion, and that two ions are present in the ion channel at a given time instant. Let their position vectors be \mathbf{x}_1 and \mathbf{x}_2 , respectively and let $U_\theta(\mathbf{x}_1, \mathbf{x}_2)$ denote the PMF of this two-ion channel. This two ion PMF can be broken down as follows:

$$U_\theta(\mathbf{x}_1, \mathbf{x}_2) = U_\theta(\mathbf{x}_1) + U_\theta(\mathbf{x}_2) + U_I(\mathbf{x}_1, \mathbf{x}_2)$$

where $U_\theta(\mathbf{x}_1)$ and $U_\theta(\mathbf{x}_2)$ denote the single ion PMF and U_I denotes the interaction term between the two ions. In a similar manner, if three ions are present in the ion channel,

$$U_\theta(\mathbf{x}_1, \mathbf{x}_2, \mathbf{x}_3) = U_\theta(\mathbf{x}_1) + U_\theta(\mathbf{x}_2) + U_\theta(\mathbf{x}_3) + U_I(\mathbf{x}_1, \mathbf{x}_2) \\ + U_I(\mathbf{x}_1, \mathbf{x}_3) + U_I(\mathbf{x}_2, \mathbf{x}_3) + U_{I3}(\mathbf{x}_1, \mathbf{x}_2, \mathbf{x}_3)$$

where U_I denotes the pairwise interaction between any two of the three ions, and $U_{I3}(\mathbf{x}_1, \mathbf{x}_2, \mathbf{x}_3)$ is the triple ion interaction. We assume that U_{I3} (and any higher order interactions in the case of more than three ions) is zero. Thus the general formula for a multi-ion PMF is

$$U_\theta(\mathbf{x}_1, \mathbf{x}_2, \dots, \mathbf{x}_n) = \sum_{i=1}^n U_\theta(\mathbf{x}_i) + \sum_{i,j=1; i \neq j}^n U_I(\mathbf{x}_i, \mathbf{x}_j)$$

The single ion PMF can be parameterized as described above, but the interaction potential still needs to be estimated. The interaction potential can be described by a two-dimensional PMF, with a functional form and initial guess based on that described above, but subject to modification by the adaptive controlled Brownian dynamics algorithm. The parameters of the interaction potential would be added to the set of possible parameters θ to be optimized, and the process would be exactly as described in the rest of the paper, only with a larger set of parameters.

3.4. PMF Estimation as a Stochastic Optimization Problem: Adaptive Controlled Brownian Dynamics

We will estimate the PMF U_θ parameterized by θ , by computing the θ that optimizes the fit between the mean current $I^{(\theta, \lambda)}$ (defined above in Eq. (8)) and the experimentally observed current $y(\lambda)$ defined below. Unfortunately, it is impossible to explicitly compute $I^{(\theta, \lambda)}$ from Eq. (8). For this reason we resort to a *stochastic optimization problem*

formulation below, where consistent estimates of $I^{(\theta, \lambda)}$ are obtained via the Brownian dynamics algorithm. The main algorithm presented in this section is the adaptive controlled Brownian dynamics simulation Algorithm 1 which solves the stochastic optimization problem and yields the optimal PMF.

The Brownian dynamics simulation algorithm is run in batches indexed by batch number $n = 1, 2, \dots$. In each batch n , the PMF parameter θ_n is selected (as described below), a number of external potentials λ at various ionic concentrations $[K]$ are applied, and the Brownian dynamics algorithm is run over L iterations. The estimated current $\hat{I}_n^{(\theta, \lambda)}$ is then computed using Eq. (8). In estimating the PMF with our adaptive Brownian dynamics algorithm, we typically use 12 target currents $y(\lambda)$ distributed across 4 different concentrations $[K]$.

Knowing that the current in the gramicidin-A channel, at a given concentration $[K]$ increases linearly with potential λ , we can model the true current as $y(\lambda, [K]) = \hat{a}([K])\lambda$, within a range of voltages ($\lambda \in [\lambda_1, \lambda_2]$), where $\hat{a}([K])$ is unknown. Assuming that the experimentally recorded currents at concentration $[K]$ closely approximate the true current, we can now seek the straight line that best fits the data available to us. Equivalently we want to find its slope (the conductance)

$$\hat{a}([K]) = \arg \min_a \sum_{\lambda \in \Lambda_{[K]}} (y(\lambda) - a\lambda)^2 \quad (14)$$

Similarly, we can find the straight line that best fits the simulated data available to us at batch n , i.e., $\hat{I}_n^{(\theta, \lambda)}$

$$\hat{d}_n(\theta, [K]) = \arg \min_d \sum_{\lambda \in \Lambda_{[K]}} (\hat{I}_n^{(\theta, \lambda)} - d\lambda)^2 \quad (15)$$

where $\cup_{[K] \in \mathcal{C}} \Lambda_{[K]} = \Lambda$ and \mathcal{C} is the set of concentrations at which potentials are applied to obtain experimental readings on the current. This leads to the following evaluated loss function, measuring the mean square error between the line derived from the experimental current and the one derived from the simulated Brownian dynamics current at a fixed concentration $[K]$:

$$\begin{aligned} \mathcal{Q}_n(\theta, [K]) &= \int_{\lambda_{1,[K]}}^{\lambda_{2,[K]}} (\hat{d}_n(\theta, [K])\lambda - \hat{a}([K])\lambda)^2 d\lambda \quad (16) \\ &= \frac{\lambda_{2,[K]}^3 - \lambda_{1,[K]}^3}{3} (\hat{d}_n(\theta, [K]) - \hat{a}([K]))^2 \quad (17) \end{aligned}$$

where $\lambda_{1,[K]}$ and $\lambda_{2,[K]}$ are the smallest and largest applied potentials at concentration $[K]$, respectively. We can now rewrite the loss function as

$$\mathcal{Q}(\theta, [K]) = \mathbf{E}\{\mathcal{Q}_n(\theta, [K])\}, \quad \mathcal{Q}(\theta) = \sum_{[K] \in \mathcal{C}} w_{[K]} \mathcal{Q}(\theta, [K]) \quad (18)$$

where $w_{[K]}$ are weights that we can manually assign to the different available concentrations at which we have values

for the current. Generally, one may want to assign different weights to the different concentration levels based, for example, on a subjective assessment of the quality of data or the number of recordings available. Finally, the optimal PMF U_{θ^*} is determined by the parameter θ^* that minimizes the above loss function, i.e., $\theta^* = \arg \min_{\theta \in \Theta} \mathcal{Q}(\theta)$.

3.5. Discrete Optimization: Conservative Stochastic Search Algorithm for Estimating the PMF

A feasible approach to solving the optimization problem presented above is to use discrete optimization. Here, the aim is to utilize an efficient optimization algorithm for computing the best PMF parameters from a discrete set of candidates. We present a *conservative* stochastic search algorithm, motivated by the work of Krishnamurthy et al.,¹⁴ where the state of the algorithm becomes more and more conservative as time moves on and converges almost surely to the optimal state. This is achieved by utilizing the average currents $\hat{I}_n^{(\theta, \lambda, \text{mean})}$ and $\hat{I}_n^{(\hat{\theta}, \lambda, \text{mean})}$ at each concentration and voltage. This average is calculated over all the visits to both the current state and the alternative state including the latest batch. Hence we define Θ_d as follows

$$\Theta_d = \{\theta_i: W_i \in [0, 30 \text{ \AA}], \quad \sigma_i^2 \in [0, \sigma_{\max}^2], \quad m_i \in [0, M], \\ \sigma_{0,i}^2 \in [0, \sigma_{\max}^2], \quad m_{0,i} \in [0, M]\} \quad (19)$$

where $i = 1, 2, \dots, S$ and $S = \#\Theta_d$ the cardinality of the set of parameters. The optimization problem becomes

$$\theta^* = \arg \min_{\theta \in \Theta_d} \mathcal{Q}(\theta) \quad (20)$$

Moreover, the algorithm described in this section is recursive and requires batch Brownian dynamics indexed by batch number $n = 1, 2, \dots$ as before. In the algorithm, θ_n denotes the *state* at batch n associated with a neighborhood $\mathcal{N}_{\theta_n} = \Theta_d - \{\theta_n\}$. Also $e_m, m = 1, 2, \dots, S$ is a S dimensional unit vector with one at the m th dimension and zeros elsewhere. The aim of discrete stochastic approximation is to devise an efficient adaptive search allowing us to find θ^* , the optimal solution, with as few Brownian dynamics (samples) as possible by not making unnecessary observations at non-promising values of θ .¹⁵ With those goals in mind, we now present the following algorithm.

Algorithm 1. Conservative Stochastic Search Adaptive Brownian Dynamics Algorithm for PMF Estimation

Redefine the loss function by replacing $\hat{I}^{(\theta, \lambda)}$ with $\hat{I}^{(\theta, \lambda, \text{mean})}$ in Eq. (15).

- *Step 0 (Initialization)*: Set batch index $n = 0$, initialize $\theta_0 \in \Theta_d$ randomly, initialize the state occupation probabilities $\pi_0 = \mathbf{e}_{\theta_0}$, and initialize the optimal state $\theta^* = \theta_0$. Initialize the S -dimensional vector \mathbf{K} to one.
- *Step 1 (Sampling and Evaluation)*: At batch n , evaluate loss function $\mathcal{Q}_n(\theta_n)$ by conducting Λ independent

Brownian dynamics simulation runs. Generate an alternative state $\tilde{\theta}_n$ by sampling uniformly from \mathcal{N}_{θ_n} and evaluate $\mathcal{Q}_n(\tilde{\theta}_n)$. Update the occupation times and the estimates of the mean currents

$$K(\theta_n) = K(\theta_n) + 1, \quad K(\tilde{\theta}_n) = K(\tilde{\theta}_n) + 1 \quad (21)$$

$$K(\theta_n)\hat{I}_n^{(\theta_n, \lambda, \text{mean})} = (K(\theta_n) - 1)\hat{I}_{n-1}^{(\theta_n, \lambda, \text{mean})} + \hat{I}_n^{(\theta, \lambda)}, \quad \hat{I}_0^{(\theta, \lambda, \text{mean})} = 0 \quad (22)$$

$$K(\tilde{\theta}_n)\hat{I}_n^{(\tilde{\theta}_n, \lambda, \text{mean})} = (K(\tilde{\theta}_n) - 1)\hat{I}_{n-1}^{(\tilde{\theta}_n, \lambda, \text{mean})} + \hat{I}_n^{(\tilde{\theta}, \lambda)}, \quad \hat{I}_0^{(\tilde{\theta}, \lambda, \text{mean})} = 0 \quad (23)$$

- *Step 2 (Conditional Acceptance)*: If $\mathcal{Q}_n(\tilde{\theta}_n) < \mathcal{Q}_n(\theta_n)$, set $\theta_{n+1} = \tilde{\theta}_n$, otherwise set $\theta_{n+1} = \theta_n$.
- *Step 3 (Occupation Probabilities Update)*: Update empirical state occupation probabilities:

$$\pi_{n+1} = \pi_n + \mu_n(e_{\theta_{n+1}} - \pi_n), \quad \pi_0 = e_{\theta_0}, \quad \mu_n = 1/n \quad (24)$$

- *Step 4 (Update Estimate of PMF)*: $\theta_n^* = \theta_{m^*}$ where $m^* = \arg \max_{m \in \{1, 2, \dots, K\}} \pi_{n+1}(m)$
- *Step 5*: Set n to $n + 1$ and go to Step 1.

It is noteworthy that Algorithm 1 is conservative since acceptance of a state is based on the average currents calculated over the batches of Brownian dynamics simulations run using the parameters of that state. Moreover, the algorithm converges with probability one because the Brownian dynamics algorithm provides unbiased estimates of the currents for the different states at each batch. Thus, by the strong law of large numbers, and for any $\theta \in \Theta_d$,

$$\lim_{n \rightarrow \infty} \hat{I}_n^{(\theta, \lambda, \text{mean})} = \mathbf{E}\{\hat{I}^{(\theta, \lambda)}\} = I^{(\theta, \lambda)} \quad (25)$$

4. RESULTS

Consider the parameterization $\theta = (W, \sigma^2, m, \sigma_0^2, m_0)'$ defined in Eq. (11) for the PMF U_θ . Since the position of the potential wells for the gramicidin-A channel are known to be around -9 \AA and $+9 \text{ \AA}$,^{9, 11, 12, 16} we fix the components $W = 9$, $\sigma^2 = 16$, and $\sigma_0^2 = 12.25$ in θ . In our numerical study, we have assumed, for simplicity, prior knowledge of the position and number of binding sites. Note that this assumption is not essential since our algorithm can also estimate these parameters. Thus, our aim is to estimate the two components (m, m_0) which determines the depth of the two potential wells of the gramicidin-A channel and the height of the potential barrier between the wells. This is obtained by estimating the parameter θ^* that optimizes the fit between the Brownian dynamics simulated current and experimentally determined current. We thus construct

Θ_d to contain 25 possible values for (m, m_0) corresponding to well depth $\in \{5 kT, 6 kT, 7 kT, 8 kT, 9 kT\}$ and barrier height $\in \{4 kT, 4.5 kT, 5 kT, 5.5 kT, 6 kT\}$. The particular values of these parameters were chosen after a preliminary study showed that choices of well-depth and barrier-height outside the given range lead to significant degradation in performance; we thus find the best fit PMF from this subset which comprises a reasonable range of values.

The experimentally determined current $y(\lambda)$ is evaluated at 12 different voltages and concentrations on the current-voltage-concentration profiles of the gramicidin-A channel. The concentration-voltage pairs used cover voltages ranging from 25–200 mV at a concentration of 500 mM as well as concentrations ranging from 100–1000 mM at voltages of 100 mV and 200 mV. Specifically, the conditions we used are 25, 50, 75, 100, 150, and 200 mV from the current-voltage curve obtained with an ionic concentration of 500 mM; 100, 200, 500, and 1000 mM from the current-concentration curves obtained with the applied potentials of 100 mV and 200 mV.

4.1. Conservative Search

The adaptive controlled Brownian dynamics simulation algorithm (Algorithm 1) is run to estimate θ^* . Figure 3 shows the evolution of the estimates $\{\theta_k^*\}$ versus batch index $n = 0, 1, \dots$. While we let the algorithm run for 100, batches, with each batch corresponding to $0.8 \mu\text{s}$, in order to verify that it has indeed converged, Figure 3 shows that convergence to the optimal state $\theta^{(7)}$ corresponding to (well depth, barrier height) = $(6 kT, 4.5 kT)$ occurs within 30 batches. In Figure 2, we plot the PMF estimate

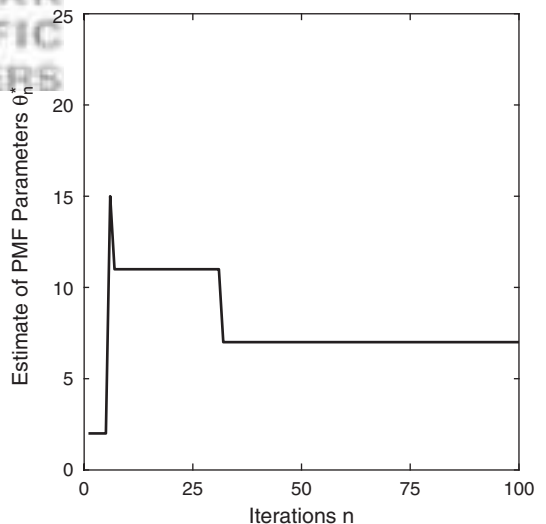
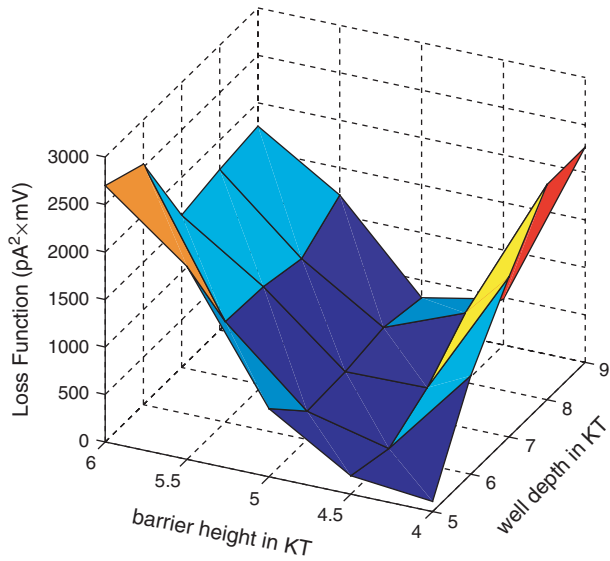
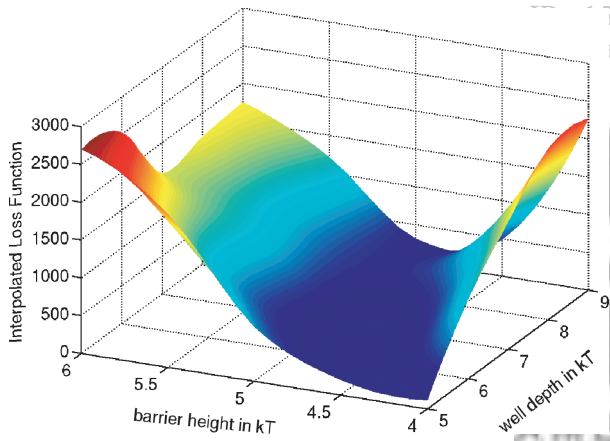


Fig. 3. Convergence of PMF Estimation Algorithm 1. The algorithm arrives at the optimal PMF (candidate 7) with barrier height $4.5 kT$ and well depth $6 kT$ within 30 iterations and is thus substantially less costly than the brute force approach as it requires a much smaller number of BD simulations, each one run for a shorter period of time.



(a) Error Surface using Algorithm 1



(b) Interpolated Version

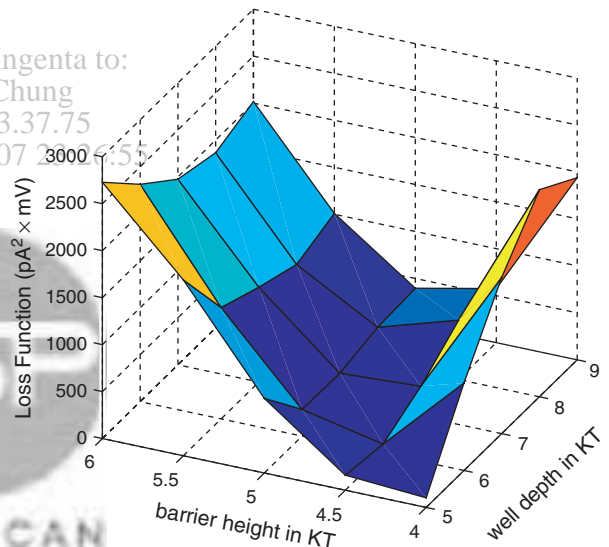
Fig. 4. The estimated error surface $\mathcal{Q}(\theta)$ of Eq. (18) obtained using Algorithm 1 (the conservative search algorithm), as well as an interpolated version of this error surface. Note that the error surface obtained using this method closely resembles the true one obtained using the brute force approach, with the estimate arrived at using a much shorter computation time. The minimum here as well occurs at a well depth of 6 kT and barrier height of 4.5 kT . Several near optimal values can be seen as well.

$U_\theta(\theta_{60})$ obtained after 3 batches of running Algorithm 1 as well as the optimal PMF.

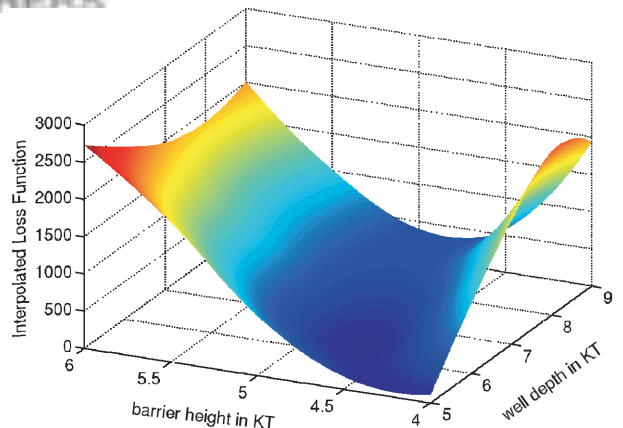
Moreover, Figure 4 illustrates the profile of the loss function obtained using Algorithm 1 with the varying well-depths and barrier heights in Θ_d as well as an interpolated version of this surface. The figure shows that the optimal value for the loss function (in dark blue), occurs at well depth and barrier height of 6 kT and 4.5 kT as mentioned previously. It also suggests that there are several possible PMF parameter values that produce near optimal values for the loss function.

4.2. Exhaustive Search

To illustrate experimentally the success of the optimization algorithm in converging to θ^* , the optimal parameters of the parameterized PMF, we run the Brownian dynamics program for an extended number of steps (corresponding to 16 μs) at each of the 25 candidate parameters $\theta \in \Theta_d$ and for the 12 various experimental conditions $\lambda \in \Lambda$. We use Brownian dynamics simulations to generate estimates of $\mathcal{Q}(\theta, [K])$, where $\theta \in \Theta_d$ and $[K] \in \mathcal{C}$. We then calculate $\mathcal{Q}(\theta)$ and plot the resultant estimate of this loss function for the various values of the well depth and barrier height along with an interpolated version in Figure 5. Recalling that our objective is to find the parameters θ^* that minimize $\mathcal{Q}(\theta)$, we arrive to well depth = 6 kT and barrier height = 4.5 kT as the optimal configuration. This



(a) True Error Surface



(b) Interpolated Version

Fig. 5. The true error surface $\mathcal{Q}(\theta)$ of Eq. (18) obtained by running all the candidate PMF's, as well as an interpolated version of this error surface. The optimal value occurs at a well depth of 6 kT and barrier height of 4.5 kT , though several near optimal values exist.

result, arrived at via a brute force exhaustive search technique exactly matches the result of the proposed discrete optimization algorithm.

4.3. Comparison of Resultant Loss Function

The values of the θ that produce a small value for the loss function in the brute-force exhaustive search approach, i.e., those corresponding to (well depth, barrier height) pairs of (5 kT, 4 kT), (5 kT, 4.5 kT), (6 kT, 4.5 kT), (6 kT, 5 kT) as well as (7 kT, 5 kT) and (8 kT, 5 kT) are the same values of θ that produce large $\pi(\theta)$ in Algorithm 1. $\pi(\theta)$ denotes the proportion of time the algorithm spends in evaluating a chosen parameter of the profile. Moreover, the values of $\pi(\theta)$ that resulted from Algorithm 1 can be seen, by comparing Figure 4 and Figure 5, to closely resemble the estimate of the loss function obtained by running the brute force approach.

In conclusion, the discrete optimization algorithm proposed was capable of converging to the optimal parameters in a relatively small number of iterations and with much lower use of computer time than the brute force approach. For the simulation setup we used, the brute force approach required running the Brownian dynamics program for 25 candidate parameters and 12 experimental points, with each simulation corresponding to 16 μ s. On the other hand, the adaptive controlled Brownian dynamics scheme required running the program for 30 iterations each with 2 candidate parameters at 12 experimental points, with each simulation corresponding to 0.8 μ s. In other words, the proposed scheme requires only 12% of the computer time used by the brute force approach.

5. DISCUSSION

We provide a novel computational scheme, which we call adaptive controlled Brownian dynamics, for estimating the PMF encountered by a permeating ion across an ion channel that does not require explicit knowledge of an effective dielectric constant and that is much less computationally expensive than an exhaustive search on a large grid of parameters. We make an initial, reasonable guess of a PMF, representing it by, for example, a mixture of Gaussian basis functions. The currents under various conditions are calculated in parallel using Brownian dynamics simulations. Typically, we select twelve points from the conductance-concentration curves and current-voltage curves. For the gramicidin-A channel, we make use of the fact that the PMF has two prominent wells near the entrance of the pore that is separated by a central barrier. At each selected voltage or concentration value, the currents under each condition is estimated with Brownian dynamics runs using an initial PMF. Then another batch of Brownian dynamics runs is carried out with different well-depth and barrier-height selected randomly from a finite discrete set of candidates. Thus 24 runs altogether,

are carried out in parallel at each iteration. After the completion of the first iteration, the currents obtained from Brownian dynamics simulations are compared with the experimental currents. To this end we use a loss function that makes explicit use of the prior knowledge we have on the gramicidin-A channel, namely that current-voltage curves are linear for a given concentration. Thus, the PMF that generates the current that better matches the experimental data is kept while the other one is replaced with a randomly selected PMF. This process is repeated many times until the estimated profiles converge.

Analysis of numerical results: In the numerical example we show for the gramicidin-A channel, the PMF that accurately replicate the experimental observations, when incorporated into a Brownian dynamics algorithm, has two wells of 6 kT in depth and an intervening barrier of 4.5 kT in height. The well depth here refers to the zero potential in the reservoir and the barrier height is measured with respect to the well minimum. Previously, Edwards et al.⁷ estimated the shape of the potential profile using the brute-force inverse method. The depth of the wells and the height of the barrier they quote are, respectively, 8 kT and 5 kT. It is of interest to compare these profiles with those obtained by Chiu and Jakobsson.¹⁷ They replicated the conductance properties of Na⁺ ions via electro-diffusion equations using a profile with the well depth of 5.4 kT and the barrier height of 4.2 kT. McGill and Schumaker¹⁸ also find that similar well depths and barrier heights are required to match experimental currents using their diffusion theory. Thus, the previous estimates of the parameters set, obtained by using a variety of different methods, are reasonably congruent to those obtained with the technique we propose here. Furthermore, all these results match well with the fact that according to Figures 4 and 5, there are several possible well-depths and barrier-heights that produce 'good' fits to the experimentally measured currents. These well-depths and barrier-heights all fall within 2 kT of the optimal well depth of 6 kT and 1 kT of the optimal barrier height of 4.5 kT that we report.

To ascertain that the optimal parameters generated by our scheme are correct, we checked our results using an exhaustive search BD and compared them with those obtained with the adaptive BD algorithm (see Figs. 4 and 5). Both approaches yield the optimal PMF with the same well-depth and barrier-height. However, several other PMF's with low values of the loss function are also uncovered, indicating that possibly more than one set of parameters can produce conduction that fits the observables well. We note here that, in estimating the parameters of the PMF, we have only attempted to match the current-voltage relationship at one concentration (500 mM) and two current concentration curves obtained with a driving voltage of 100 mV and 200 mV. If more available data sets are used in evaluating the loss function, it is likely that the optimal parameters will converge on one value. For example, the binding constant K_d of ions in the two

binding sites is known, but we have not made use of this information in assessing the loss function.

Discrete stochastic optimization for PMF estimation: There are several methods that can be utilized in refining the initially guessed PMF through successive iterations. To avoid explicit computation of the Hessian, we make use of discrete stochastic optimization algorithms. The basic stochastic optimization procedure starts out with an initial guess at the PMF, and this initial guess is updated on an iteration-by-iteration basis with the aim of improving the fit between the simulated currents and the experimental data. Minimizing the discrepancies between these two sets of quantities involve adjustments of several variables. In the simple test case we use in this paper, the PMF is represented with a mixture of three Gaussian functions, optimization involving the adjustment of only two parameters. We have used discrete optimization over a set of 25 different combinations of well-depth and barrier-heights. Alternatively, one can use continuous optimization, utilizing for example the Kiefer-Wolfowitz finite difference gradient estimator.

Applicability to other ion-channels: The method detailed here, we note, can be applied to any ionic channel, in which conduction takes place as a single or multi-ion process. If, for example, the pore is occupied by two or more ions and conduction takes place as a ‘knock-on’ effect, as it does in the L-type calcium channel¹⁹ and the KcsA potassium channel,^{20,21} we first need to estimate the PMF for a single ion permeating across the pore, as it is done for the gramicidin-A channel. Multiple ions attracted to the pore will exert the forces on each other via the repulsive Coulomb force and induced surface charges on the protein–water interface. These two components of the forces, tabulated in a ‘lookup’ table, need to be added to the PMF. Because the construction of such a table requires an assumed value of ϵ_c , one could construct many such tables, each with a different value of ϵ_c , and then select

one that minimizes the ‘loss function,’ and the estimated PMF converges most rapidly. One could alternatively utilize a parameterized multi-ion PMF, i.e., with no explicit use of ϵ_c as we did with the single ion PMF, and then solve an optimization problem to extract the multi-ion PMF parameters.

References

1. M. B. Partenskii and P. C. Jordan, *J. Phys. Chem.* 96, 3906 (1992).
2. M. B. Partenskii and P. C. Jordan, *Q. Rev. Biophys.* 25, 477 (1992).
3. O. S. Andersen and R. E. Koeppel, *Phys. Rev.* 72, 89 (1992).
4. D. D. Busath, *Annu. Rev. Physiol.* 55, 473 (1993).
5. R. E. Koeppel and O. S. Andersen, *Annu. Rev. Biophys. Biomol. Struct.* 25, 231 (1996).
6. B. A. Wallace, *J. Struct. Biol.* 121, 123 (1998).
7. S. Edwards, B. Corry, S. Kuyucak, and S. H. Chung, *Biophys. J.* 83, 1348 (2002).
8. V. Krishnamurthy and S.-H. Chung, *IEEE Trans. Nanobiosci.* 5, 126 (2006).
9. B. Roux and M. Karplus, *J. Am. Chem. Soc.* 115, 3250 (1993).
10. B. Roux and M. Karplus, *Annu. Rev. Biophys. Biomol. Struct.* 23, 731 (1994).
11. T. W. Allen, T. Bastug, S. Kuyucak, and S. H. Chung, *Biophys. J.* 84, 2159 (2003).
12. T. W. Allen, O. S. Andersen, and B. Roux, *Proc. Natl. Acad. Sci. USA* 101, 117 (2004).
13. T. W. Allen, O. S. Andersen, and B. Roux, *J. Gen. Physiol.* 124, 679 (2004).
14. V. Krishnamurthy, X. Wang, and G. Yin, *IEEE Trans. Information Theory* 50, 1927 (2004).
15. G. Pflug, *Optimization of Stochastic Models: The Interface Between Simulation and Optimization*, Kluwer Academic Publishers (1996).
16. F. Tian and T. A. Cross, *J. Mol. Biol.* 285, 1993 (1999).
17. S. W. Chiu and E. Jakobsson, *Biophys. J.* 55, 147 (1989).
18. P. McGill and M. F. Schumaker, *Biophys. J.* 71, 1723 (1996).
19. B. Corry, T. Allen, S. Kuyucak, and S. H. Chung, *Biophys. J.* 80, 195 (2001).
20. D. A. Doyle, J. M. Cabral, R. A. Pfuetzner, A. Kuo, J. M. Gulbis, S. L. Cohen, B. T. Chait, and R. MacKinnon, *Science* 280, 69 (1998).
21. S. H. Chung, T. Allen, and S. Kuyucak, *Biophys. J.* 82, 628 (2002).

Received: 24 May 2006. Accepted: 29 May 2006.